Beyond ^{132}Sn

Examples of new data on exotic neutron-rich Te isotopes from fission and β-decay

Radomira Lozeva[1,*], *Min* Si[1], and *Guillaume* Häfner[1,2]

[1]CSNSM, CNRS/IN2P3, Université Paris-Saclay, F-91405 Orsay Campus, France
[2]IKP, Universität zu Köln, D-50937 Köln, Germany

Abstract. Exotic nuclei beyond the ^{132}Sn double shell-closure have both single-particle and collective particle-hole excitations and are expected to have competing excitation patterns from both type of excitations together with possible structural changes. We are, therefore, studying the region in the close vicinity beyond ^{132}Sn and further with the neutron increase with experimental methods such as induced fission and β decay. A short overview of this knowledge will be given together with examples of newly obtained data at preliminary stage.

1 Introduction and Motivation

Exotic nuclei beyond the ^{132}Sn double shell-closure are influenced by both the Sn superfluity and the evolving collectivity only a few nucleons away, involving predominantly protons from the lower-lying $\pi g_{7/2}$ and $\pi d_{5/2}$ orbitals and the neutrons in the $\nu f_{7/2}$, $\nu p_{3/2}$ and $\nu h_{9/2}$ orbitals beyond, respectively, Z=50, N=82 closed shells. For neutron-rich nuclei, for example at intermediate mass number A~136, the interplay between single-particle and collective particle-hole excitations [1, 2] is evident in mid-shell $\nu f_{7/2}$. On the other hand at the end of the $\nu f_{7/2}$ shell possible sub-shell gap with respect to $\nu p_{3/2}$ has been suggested [3]. With the extreme addition of neutrons but also protons additional effects are expected such as the formation of neutron skin [4], orbital crossings between $\pi g_{7/2}$ and $\pi d_{5/2}$ orbitals [5, 6] and possible quickly evolving deformation [7].

The knowledge of experimental nuclear ingredients is especially interesting beyond ^{132}Sn as little is known on how the excitation modes develop with the addition of both protons and neutrons for the Sb, Te, I nuclei. Therefore, systematic prompt and decay studies can be such a sensitive probe for their structure [8, 9]. Aiming at more global picture and understanding this barely explored neutron-rich portion of the nuclear chart, we have performed several investigations, recently.

We have produced the nuclei of interest following fission such as relativistic ^{238}U on ^{9}Be in inverse kinematics, thermal neutron-induced fission on ^{241}Pu and ^{235}U or fast neutron-induced fission on ^{238}U and ^{232}Th and in β-decay of fission products in several recent γ-ray spectroscopy projects [8–10]. Consistent data analysis allows to access various spins and excitation energies and to provide complementary data, better understanding, as well as a new and indispensable input to theory. Examples from some of these studies on isotopes with A~136 will be briefly presented along with a short discussion of the new data. Detailed description and further details will be accordingly published in dedicated articles [11, 12].

2 New data on ^{134}Te from fission

With only two valence protons outside the doubly-magic ^{132}Sn, a long-lived isomeric J = 6 state emerges in ^{134}Te based on the $\pi g^2_{7/2}$ proton configuration. Below the 6^+_1 isomer, a short-lived 4_1+ isomer with $T_{1/2}$ = 1.28(10) ns has been observed [13]. The nucleus of interest has been produced in a fast neutron-induced fission experiment and its de-excitation measured with a hybrid array consisting of HpGe and $LaBr_3$(Ce) scintillation detectors [10].

Due to its short half-life, the 4^+_1 state is not measurable with HpGe detectors, but delayed $LaBr_3$(Ce), after tagging the ^{134}Te nucleus can be utilized for measuring this state. In the left panel of Fig. 1, the $LaBr_3$(Ce) energy projection can be seen after gating on the 1279 keV $2^+_1 \rightarrow 0^+_1$ transition and several transitions above the 6^+_1 isomer. Both, 115 and 297 keV transitions feeding and de-populating the 4^+_1 state are visible. Furthermore, the $LaBr_3$(Ce) projection after an additional $LaBr_3$(Ce) gate on 115 keV is shown. The time difference spectrum, illustrated in the right panel of Fig. 1 has been fitted with an exponential decay curve plus constant background to obtain the half-life, $T_{1/2}$. A value of $T_{1/2}$ = 1.3(3) ns has been obtained, in accordance with the literature value of 1.36(11) ns [14]. This measurement demonstrates the feasibility of measuring ns and sub-ns lifetimes with this experiment and is employed toward more neutron rich Te isotopes of interest.

3 New data on ^{136}Te from fission

The neutron rich ^{136}Te has two valence protons and neutrons outside the doubly magic ^{132}Sn and is of major importance to study the onset of collectivity beyond the ^{132}Sn

*e-mail: radomira.lozeva@csnsm.in2p3.fr

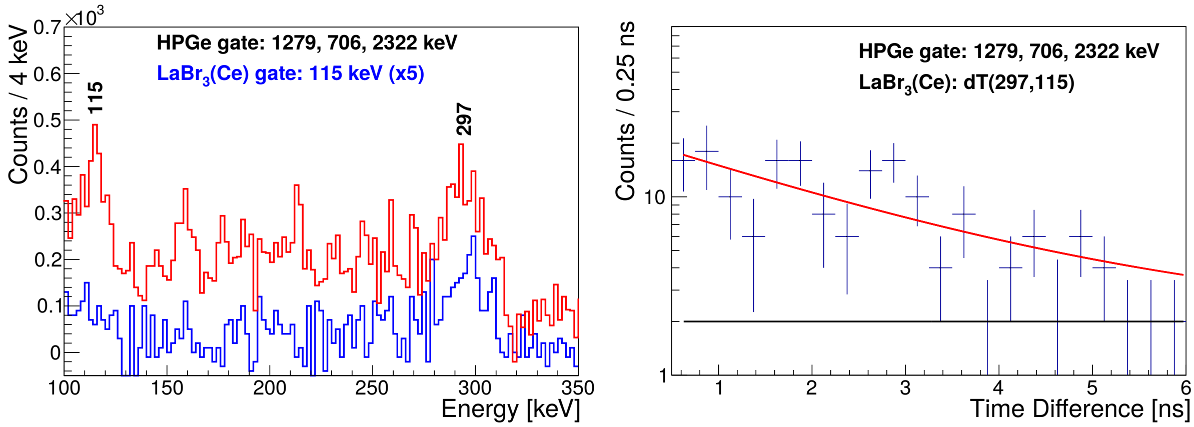

Figure 1. Left: Delayed LaBr$_3$(Ce) energy projection after applying a HpGe gate on several transitions in ^{134}Te (red) and an additional LaBr$_3$(Ce) gate on 115 keV (blue). Right: Time difference of the 297 - 115 keV cascade to measure the half-life of the 4_1^+ state in ^{134}Te. The distribution was fitted using an exponential decay (red) plus a constant background (black).

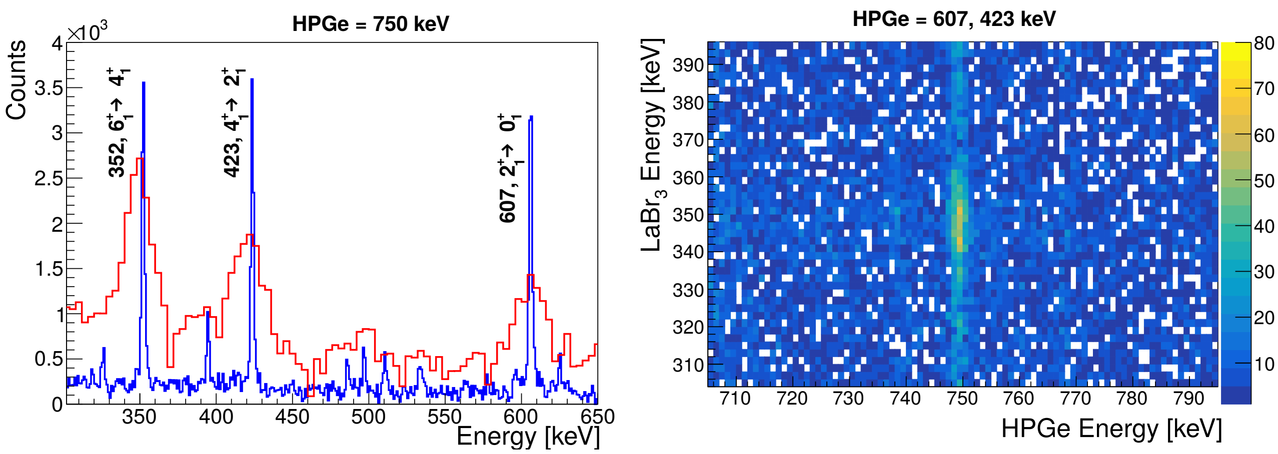

Figure 2. Left: Prompt energy projection after applying a HpGe gate on the 750 keV transition in ^{136}Te. The LaBr$_3$(Ce) energy spectrum is shown in red and the HpGe spectrum in blue. The strongest transitions from ^{136}Te are labeled with their respective energies. Right: LaBr$_3$(Ce) - HpGe energy matrix after gating on the two lowest transitions in ^{136}Te. The zoomed area corresponds to the 750 - 352 keV coincidence.

core. Excited states in ^{136}Te have been populated in fast neutron-induced fission and its γ-rays detected using the previously described (see Section 2) combination of HpGe and LaBr$_3$(Ce) scintillation detectors.

Figure 2 shows an example for the ^{136}Te nucleus. In the left panel of Fig. 2, the energy projection after applying a clean HpGe gate on the 750 keV, $8_1^+ \rightarrow 6_1^+$ transition in ^{136}Te is presented. All the transitions below the 6_1^+ are clearly visible in both LaBr$_3$(Ce) and HpGe energy projections. Utilizing the superior energy resolution of the HpGe detectors one can conclude that the peaks of interest show almost no contribution from other contaminants. From measuring time differences between the labeled transitions, lifetimes of the respective states are deduced.

In the right panel of Fig. 2 an energy matrix is shown to demonstrate the HpGe - LaBr$_3$(Ce) coincidence between the $8_1^+ \rightarrow 6_1^+$ and $6_1^+ \rightarrow 4_1^+$ transition in ^{136}Te. The number of coincidence counts amounts to about 10^3 which, scaled by efficiencies for the LaBr$_3$(Ce), is reasonable to measure the lifetime of the 6_1^+ state in ^{136}Te. This data result will be presented in a forthcoming article [12].

4 New data on ^{136}Te from β decay of ^{136}Sb

The β-decay data of ^{136}Sb to ^{136}Te, accessing the low-spin states which are not populated in fission, is extremely scarce [14]. It gives very important information not only on the ground state spin/parity and thus its properties, but also on specific type first excited states, such as the 2_1^+, 2_2^+, 2_3^+ etc. Such measurement has been performed using β-decay of A =136 fission products after the thermal neutron-induced fission of ^{235}U and detected using a system of clover HpGe, coaxial HpGe and LaBr$_3$(Ce) detectors in combination with β-decay detectors and a tape station.

Well adapted to the lifetime of the ^{136}Sb nucleus [14], the duty cycle of the system allowed the short-lived daughter to be well separated from the grand-daughter decays

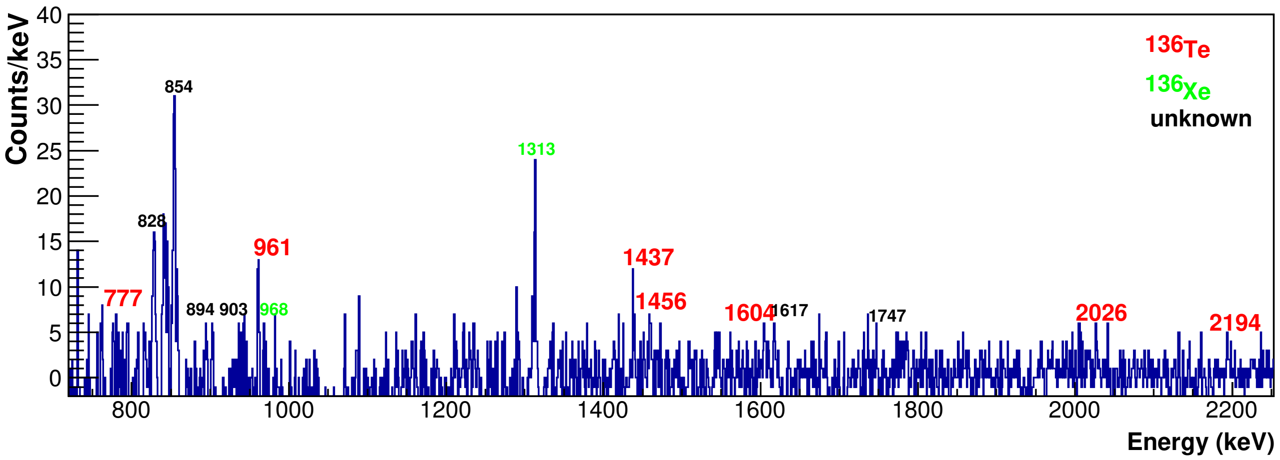

Figure 3. Short-lived energy projection corresponding to the decay of ^{136}Sb using HpGe detectors and gate on 606 $2^+_1 \rightarrow 0^+$ transition in ^{136}Te (red) and an additional anti-coincidence gate on the 1313 keV transition $2^+_1 \rightarrow 0^+$ in ^{136}Xe (green). New transitions e.g. candidates belonging to ^{136}Te are in black.

Te→I and I→Xe with the help of a chopper system. In addition, to clean-up from the strongly produced grand-daughter activities anti-coincidence gates from the grand-daughter nucleus are applied. Furthermore, long-lived activities in ^{136}I grand-daughter are also subtracted from the time window. This is demonstrated in Fig. 3, where several new candidates for the level scheme of ^{136}Te are shown. The detailed level scheme will be given together with all newly extracted *logft* values in a forthcoming article [11].

5 Discussion

The new data allows to verify and expand our current knowledge for these mid-shell nuclei (A~136) with respect to the $\nu f_{7/2}$ orbital nuclei, which is the lowest-lying neutron orbital beyond ^{132}Sn. The collected new information allows multiple coincidence relations to be established and used determine the position in the level scheme of new, or verify previously known γ transitions.

In addition, several lifetime measurements have been possible in the data analysis. Added to the new γ-ray information these provide new and important ingredients to compare with shell-model theory. The current understanding of the region with reasonably slow development of collectivity at mid-shell, expected to increase with the increase of the valence particles, can now be reexamined, especially for states which have not been populated in previous measurements. From preliminary view, the new data reasonably well agrees with the expectations from theory, however only the very detailed comparison will allow specific conclusions to be drawn [11, 12]. The experimental ingredients such as the transition rates obtained from the lifetime measurements allow better tuning of the transition matrix elements. Such data is valuable when testing the nucleon-nucleon interaction for the region beyond ^{132}Sn and when predicting nucleon or two nucleon excitations e.g. type $\pi g^2_{7/2}$ and $\nu f^2_{7/2}$ in the currently out of reach A>140 region.

In the data on the Sb β decay, for the first time a very large Q_β window has been experimentally scanned. This allows the population of many new low-spin states at high excitation energy. This, respectively, provides a field for more detailed comparison to shell-model, particularly on the strength of the first-forbidden transitions beyond ^{132}Sn. New ingredients in understanding the role of first-forbidden transitions with respect to the Gamow-Teller strength can now be analysed in details, especially as it is open in ^{136}I [8], but not seen in the Te chain [14]. Thus, combining both data sets with our previous knowledge in the region, new transitions, new excitation energies and extension of the level schemes, with new spin/parity etc. contributes importantly to the structure studies of the populated states and their behaviour beyond ^{132}Sn.

References

[1] M. -G. Porquet, S. Peru and M. Girod, Eur. Phys. J. A **25**, 319 (2005).

[2] R. Kshetri, M. Saha Sarkar, and S. Sarkar, Phys. Rev. C **74**, 034314 (2006).

[3] S. Sarkar and M. Saha Sarkar, Phys. Rev. C **81**, 064328 (2010).

[4] B. A. Brown, Phys. Rev. Lett. **85**, 5296 (2000).

[5] J. Shergur, B. A. Brown, V. Fedoseyev *et al.*, Phys. Rev. C **65**, 034313 (2002).

[6] R. Lozeva, H. Naidja, F. Nowacki *et al.*, Phys. Rev. C **93**, 014316 (2016).

[7] W. Urban, T. Rzaca-Urban, A. Korgul *et al.*, Phys. Rev. C **65**, 024307 (2002).

[8] R. Lozeva, E. A. Stefanova, H. Naidja *et al.*, Phys. Rev. C **98**, 024323 (2018).

[9] M. Jentschel, A. Blanc, G. de France *et al.*, J. Instrum. **12**, 11003 (2017).

[10] J. N. Wilsson, M. Lebois, L. Qi *et al.*, Phys. Rev. Lett. **118**, 222501 (2017).
[11] M. Si *et al.*, in preparation.
[12] G. Häfner *et al.*, in preparation.
[13] J. P. Omtvedt, H. Mach, B. Fogelberg *et al.*, Phys. Rev. Lett. **75**, 3090 (1995).
[14] www.nndc.bnl.gov